# Correlation of film thickness to optical band gap of Sol-gel derived $Ba_{0.9}Gd_{0.1}TiO_3$ thin films for optoelectronic applications

*Yen Chin* Teh[1,2] , *Ala'eddin* A. Saif [1,2*], *Zul Azhar* Zahid Jamal[1], and *Prabakaran* Poopalan[1,2]

[1]School of Microelectronic Engineering, University Malaysia Perlis, Pauh Putra Campus, 02600 Arau, Perlis Malaysia

[2]AMBIENCE UniMAP, Kompleks Kilang SME Bank, Kawasan Perindustrian Kuala Perlis, 02000 Kangar, Perlis Malaysia

**Abstract.** $Ba_{0.9}Gd_{0.1}TiO_3$ thin films have been fabricated on $SiO_2$/Si and fused silica by sol-gel method. The films are prepared through a spin coating process and annealed at 900 °C to obtain crystallized films. The effect of film thickness on the microstructure and optical band gap has been investigated using X-ray diffractometer, atomic force microscope and ultraviolet-visible spectroscopy, respectively. XRD patterns confirm that the films crystallized with tetragonal phase perovskite structure. The films surface morphology is analysed through amplitude parameter analysis to find out that the grain size and surface roughness are increased with the increase of films thickness. The transmittance and absorbance spectra reveal that all films exhibit high absorption in UV region. The evaluated optical band gap is obtained in the range of 3.67 - 3.78 eV and is found to be decreased as the thickness increase.

## 1 Introduction

Barium titanate ($BaTiO_3$) is a ferroelectric material that has gained much attention in recent decades for its excellent electrical and optical properties, and the simplicity of its crystal structure that can adapt variety types of dopant [1-2]. The incorporation of different element as dopant into $BaTiO_3$ has been extensively investigated in order to improve its original properties and extends the areas of application of barium titanate [3-4]. In spite of the fact that $Gd^{3+}$ possessed a strong influences on electrical properties with high refractive index which makes it a good candidate for optoelectronic applications [4-6].

In optoelectronics, the responsivity of the material toward light wavelength is important to define its application. As a result, many researchers have focused on tuning the material's band gap based on desired applications through variety of parameters. The thickness of perovskite oxide films plays a role as one of parameters that can influence on many properties of the films, such as transport properties, optical band gap and the electronic structure [7]. Chen *et al*. [8] reported that film quality is highly dependent on the film thickness of sputtered BFO thin films, whereby thinner film displays greater leakage current with less light absorption yet demonstrated a great photovoltaic effect. Fasasi *et al*. [9] observed changes in band gap energy by altering the thickness of Zn-$BaTiO_3$ thin films. Thus, a better understanding of the thickness effect on the film properties is essential to optimize the optoelectronic device for better performance. Among the thin films fabrication technique, Sol-gel method possessed a great advantages for its simplicity in producing high homogeneity films at low processing temperature with low cost equipment [10]. In the present work, multi-layered of $Ba_{0.9}Gd_{0.1}TiO_3$ (BGT) thin films are fabricated on $SiO_2$/Si and fused silica substrate by sol-gel technique. The effect of different thicknesses on the microstructure and optical properties of BGT films are investigated using XRD, AFM and UV-Vis spectroscopy. The correlation between the optical band gap and microstructure at different film thicknesses are also discussed in some details.

## 2 Experimental Procedures

Pre-calculated amount of barium and gadolinium acetates were dissolved in heated glacial acetic acid at constant stirring, and followed by refluxing until a clear and transparent solution was obtained. At room temperature condition, a titanium solution was prepared by mix-stirred a stoichiometric amount of titanium (IV) isopropoxide with 2-methoxyethanol. This solution was then added into Ba:Gd solution and continued in stirring at room temperature. The stirred mixture was refluxed at 120 °C to obtain a clear and homogeneous solution. The final solution is filtered and used as stock solution. The BGT thin films were fabricated by spin coating

* Corresponding author: alaeddinsaif@gmail.com

technique. The stock solution was spun-coated onto $SiO_2$/Si and fused silica substrates at 4000 r.p.m for 20s, and then followed by heating at 200 ºC for 10 minutes to vaporize the organic solvent which formed a thin film. The deposition and heating processes were repeated until desired thickness was achieved. The final as-deposited thin films were annealed at 900 ºC for 1 hour in atmosphere ambient to form crystallized films. Four samples with different thicknesses were prepared, and denoted as BGT1, BGT2, BGT3 and BGT4. In order to measure the film thickness, the films were partially etched using diluted hydrofluoric acid to create a step profile. This step profile was measured using stylus profilometer. The obtained average thicknesses of fabricated sample BGT1 to 4 were 121.215 nm, 219.556 nm, 363.890 nm and 490.398 nm, respectively. The crystal structure of the BGT films was confirmed by using X-ray diffractometer (XRD, XRD 6000, Shimadzu) with Cu-kα radiation source (λ = 1.5406 Å). Surface morphologies were characterized using a non-contact mode of atomic force microscopy (AFM, SPA 400, SII Nanotechnology, Inc) at different location away from sample edges. The optical transmittance and absorbance spectra were measured by using UV-Vis spectrometer (Perkin Elmer, LAMBDA 950) at room temperature.

## 3 Results and discussion

Fig. 1 illustrates the XRD pattern of BGT films, deposited on $SiO_2$/Si and annealed at 900 ºC. The orientation peaks (marked as P) appear in the pattern confirms the existence of perovskite structure in the films. A minor secondary phase corresponding to fresnoite (marked as f) is detected within the diffraction range. This secondary phase is attributed to the inter-diffusion between BGT films and substrate at high annealing temperature [11]. The appearance of secondary phase at 900 ºC is consistent with Huang *et al.* [12] results for $Gd_2O_3$ deposited on silicon substrate. The determined lattice constant, *a* and *c*, from the perovskite peaks are 3.9786 ± 0.0056 Å and 4.0248 ± 0.0189 Å, respectively. This indicates that the film is crystallized with tetragonal perovskite structure phase.

AFM analysis has been employed to study the surface morphology of BGT films deposited on fused silica. Fig. 2 shows the AFM three-dimensional micrographs of different thicknesses of BGT films with scanned area of 5 µm x 5 µm. These micrographs reveal the microstructure nature of the films and the behaviour of grain structure with the film thickness. It is apparently seen from the fig. that dense and smooth surfaces are obtained with grains distributed uniformly over the surface area. The grain size of distributed grain on the surface are measured and listed in Table 1. The grain size is found to be increased as the thickness increases. This increment is attributed to the grain growth during heating and annealing processes [13].

In order to further analyse the surface roughness of BGT films, amplitude parameter analysis has been performed at different point on the sample surface and the results are compiled in Table 1. From the table, both average roughness and RMS roughness increased with the increase of thickness. This increase in roughness could be due to the surface grain growth [14]. The surface asymmetry and flatness can be evaluated from the parameter of skewness and kurtosis [15]. Apparently, from the table all the samples show positive skewness surface and kurtosis surface of less than 3 indicating that all the film surfaces contain disproportionate number of peaks [16].

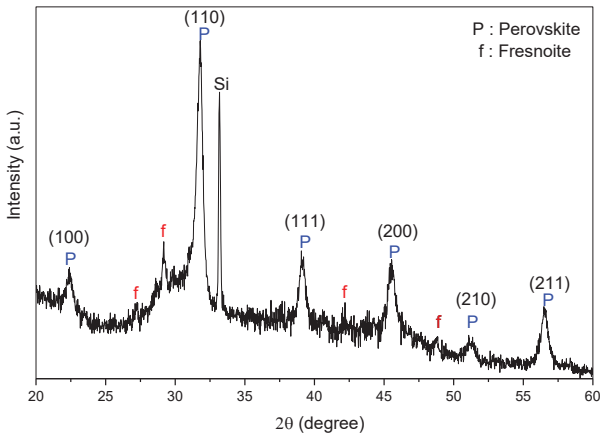


**Fig. 1.** XRD pattern of $Ba_{0.9}Gd_{0.1}TiO_3$ thin films.

Fig. 3 shows the transmittance and absorbance spectra of BGT films at different thicknesses, recorded at room temperature. It is found that the transmittance of the BGT films in the wavelength region of 350 nm to 800 nm reduces as the thickness increases as shown in fig. 3(a). This transmittance reduction has satisfies the Beer-Lambert law which is given by [17]

$$T = \exp^{(-\alpha d)} \quad (1)$$

where the intensity of transmitted light, *T*, decreases exponentially with thickness of sample, *d,* and absorption coefficient, *α*. As incident light shines through the sample, the total incident of light reduces as a result of scattering from the films. This light scattering could be due to the grain size increment and higher surface roughness [18].

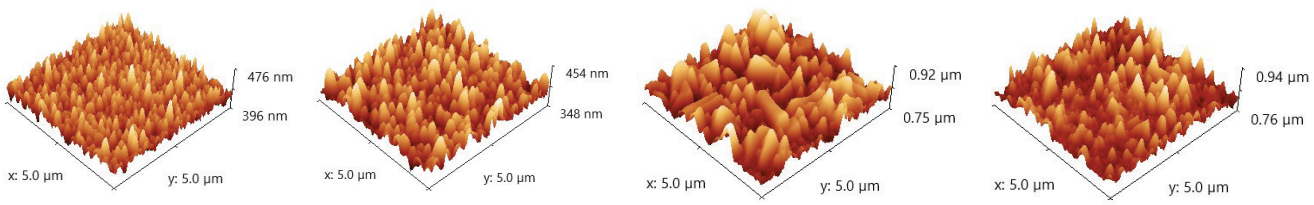


(a) (b) (c) (d)

**Fig. 2.** Three-dimensional AFM micrograph of BGT films fabricated at different thickness of (a) 121.215 nm, (b) 219.556 nm, (c) 363.890 nm and (d) 490.398 nm .

**Table 1** Amplitude parameters of BGT films at different thicknesses.

| Sample | BGT1 | BGT2 | BGT3 | BGT4 |
|---|---|---|---|---|
| Grain size (nm) | 160.522 ±3.202 | 164.594 ±3.486 | 174.794 ±3.693 | 187.4545 ±4.193 |
| Average Roughness (nm) | 7.839 ±0.078 | 11.782 ±0.085 | 19.542 ±0.405 | 15.122 ±0.410 |
| RMS Roughness (nm) | 9.7936 ±0.092 | 14.590 ±0.080 | 24.185 ±0.466 | 19.500 ±0.514 |
| Skewness | 0.2614 ±0.041 | 0.601 ±0.018 | 0.558 ±0.010 | 0.971 ±0.059 |
| Kurtosis | 0.21556 ±0.121 | 0.166 ±0.030 | 0.243 ±0.059 | 1.208 ±0.179 |

The absorbance spectra reveal the light absorption behaviour in the wavelength range of 200 nm to 800 nm. It is clearly seen that relatively low in absorbance found in the range of 350 nm to 800 nm as shown in fig. 3 (b). However, BGT films apparently have high absorption in the UV wavelength region of 200 – 350 nm as shown in fig. 3(b). It is also observed that the absorbance in this region is proportionally increased with the film thickness which could be due to film crystallinity improvement. A significant shift in cut off wavelength towards longer wavelength as the thickness increase can be observed clearly from both transmittance and absorbance spectra, which attributed to the thickness effect [19].

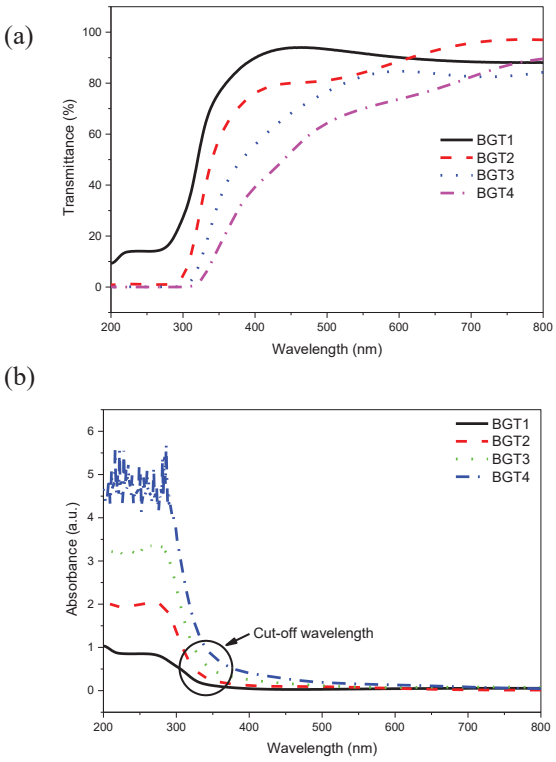


**Fig. 3.** Optical spectra, (a) transmittance and (b) absorbance, of BGT films fabricated at different thicknesses.

The optical interband transition and the value of band gap can be determined using Tauc relation which given as [20]

$$(\alpha h\nu) = B(h\nu - E_g)^m \quad (2)$$

where $h\nu$ is the photon energy, $B$ is a constant, $m$ = 1/2 and 3/2 for allowed direct and forbidden direct transitions, and $m$ = 2 and 3 for allowed indirect and forbidden indirect transitions respectively [21]. Absorption coefficient, denoted as α can be calculated from transmittance spectra which given as

$$\alpha = 1/d \ ln \ (1/T) \quad (3)$$

Thus, the optical band gap is deduced from the intercept of x-axis at zero y-axis from the plot of $\alpha h\nu^{1/m}$ against $h\nu$ through extrapolation of the linear part of the plot.

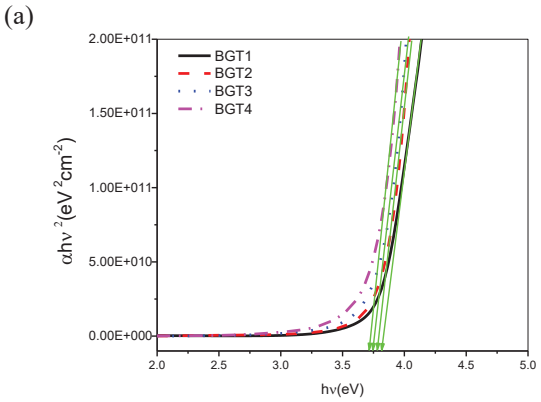

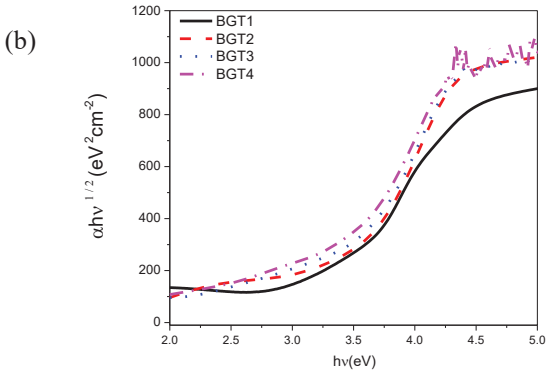


**Fig. 4.** Tauc plot of (a) $(\alpha h\nu)^2$ and (b) $(\alpha h\nu)^{1/2}$ as a function of hν of BGT films at distinct thicknesses.

In order to determine the interband transition of BGT films at different thicknesses in this work, the $\alpha h\nu^{1/m}$ with direct and indirect transition are plotted against $h\nu$ as illustrated in fig. 4 (a) and (b). By comparing both graphs, it is observed that the best fit of straight line is obtained for m = 2, indicating that direct-allowed transition takes place between valence bands and conduction bands for BGT films. The value of optical band gap for BGT1, BGT2, BGT3 and BGT4 films are found to be 3.78 eV, 3.73 eV, 3.69 eV and 3.67 eV, respectively, which are decreasing as the thickness increased. The decrement in band gap can be linked to the increment of grain size as discussed in AFM results, which is attributed to the quantum size effect, whereby the smaller the crystal size, the larger the energy band gap [22]. Similar reduction in optical band gap as the thickness increased has been reported by Zhou *et al.* [23] for BFO thin films.

## 4 Conclusions

Gadolinium doped barium titanate thin films have been fabricated on $SiO_2$/Si and fused silica by sol-gel method. The phase structure of the crystallized films obtained from XRD result confirms the existence of perovskite structure with tetragonal phase. AFM micrographs illustrate the distribution behaviour of grain over the surface as the thickness increases. The average grain size is found to be increased with the increase of film thickness, which is resulted from the grain growth mechanism during heating and annealing processes. Similar increment is observed for surface roughness with thickness increase. From the skewness and kurtosis, the films surfaces are found to be having disproportionate number of peaks and spread out distribution. Both the transmittance and absorbance spectra illustrate that all the films exhibit high absorption in the wavelength region of 200 - 350 nm. The optical band gap that determined from transmittance spectra is found to be reduced as the film thickness increases, which due to quantum size effect as correlated with the grain size of the films. Therefore, the obtained results illustrate the possible integration BGT thin films into optoelectronic devices depending on the application needs.

This work is supported by the Fundamental Research Grant Scheme (FRGS) with the Grant number 9003-0479, funded by the Ministry of Higher Education (KPT).

## References

1. Z. H. Dughaish, *Acta Phys. Pol. A*, **123**, 87 (2013)
2. Y. Huan, X. Wang, J. Fang, L. Li, *J. Eur. Ceram. Soc*., **34**, 1445 (2014)
3. A. Rani, J. Kolte, S. S. Vadla, and P. Gopalan, Ceram. Int., **42**, 8010 (2016)
4. J. P. H. Lara, M. P. Labra, F. R. B. Hernández, J. A. R. Serrano, E. O. A. Davila, P. Thangarasu, and A. H. Ramirez, *Mater. Res*., 1 (2017)
5. A. Y. Fasasi, B. D. Ngom, J. B. Kana-Kana, R. Bucher, M. Maaza, C. Theron, U. Buttner, *J. Phys. Chem. Solids*, **70**, 1322 (2009)
6. Y. Li, Y. Hao, X. Wang, X. Yao, *Ferroelectrics*, **407**, 134 (2010)
7. X. He, K.-J. Jin, C. Ge, C. Wang, H.-B. Lu, G.-Z. Yang, *J. Epl*, **102**, 37007 (2013)
8. M. Chen, J. Ding, J. Qiu, N. Yuan, *Mater. Lett.,* **139**, 325 (2015)
9. A. Y. Fasasi, M. Maaza, E. G. Rohwer, D. Knoessen, C. Theron, A. Leitch, U. Buttner, *Thin Solid Films*, **516**, 6226 (2008)
10. M. N. Kamalasanan, S. Chandra, P. C. Joshi, A. Mansingh, *Appl. Phys. Lett.*, **59**, 3547 (1991)
11. T. M. Stawski, W. J. C. Vijselaar, O. F. Göbel, S. A. Veldhuis, B. F. Smith, D. H. A. Blank, J. E. Ten Elshof, *Thin Solid Films*, **520**, 4394 (2012)
12. M. R. S. Huang, C. P. Liu, J. C. Wang, Y. K. Chen, C. S. Lai, Y. C. Fang, L. Shu, *Thin Solid Films*, **520**, 5579 (2012)
13. Y. C. Teh, A. A. Saif, Z. A. Z. Jamal, P. Poopalan, *Adv. Mater. Res.,* **911**, 251 (2014)
14. A. A. Saif, N. Ramli, P. Poopalan, *Jordan J. Phys.*, **3**, 61 (2010)
15. M. Raposo, Q. Ferreira, P. A Ribeiro, *Mod. Res. Educ. Top. Microsc.*, 758 (2007)
16. G. Yildirim, S. Bal, M. Gulen, A. Varilci, E. Budak, M. Akdogan, *Cryst. Res. Technol*., **47**, 195 (2012)
17. W. Leng, C. Yang, H. Ji, J. Zhang, J. Tang, H. Chen, *J. Mater. Sci. Mater. Electron.*, **17**, 1041–1045 (2006)
18. S. Bobby Singh, H. B. Sharma, H. N. K. Sarma, S. Phanjoubam, *Physica B: Condensed Matter*, **403**. 2678 (2008)
19. A. Singh, Z. R. Khan, P. M. Vilarinho, V. Gupta, R. S. Katiyar, *Mater. Res. Bull*., **49**, 531 (2014)
20. S. Kumari, N. Ortega, A. Kumar, J. F. Scott, R. S. Katiyar, *AIP Adv*., **4**, 37101 (2014)
21. J. Ahmad, H. Minami, S. Alam, J. Yu, Y. Arai, H. Uwe, *Chinese Phys. Lett.*, **25**, 4421 (2008)
22. K. Suzuki K. Kijima, *Jpn. J. Appl. Phys.*, **44**, 2081 (2005)
23. Y.-E. Zhou, X.-Y. Tan, B.-F. Yu, L. Liu, S.-L. Yuan, W.-H. Jiao, *Chinese Phys. Lett.*, **31**, 037304 (2014)